Macromolecular Chemistry and Physic
www.mcp-journal.d

Check for updates

Functional Silica and Carbon Nanocomposites Based on Polybenzoxazines

*Mohamed Gamal Mohamed and Shiao Wei Kuo**

The preparation of organic/inorganic hybrid materials comprising a polybenzoxazine (PBZ) matrix incorporating silicon-based species (e.g., polydimethylsiloxane [PDMS], layered silicates [clays], and polyhedral oligomeric silsesquioxanes [POSS]) and carbon-based materials (e.g., carbon black, carbon fibers, carbon nanotubes, and graphene) has received much attention in recent years because these composites display low water absorption, low surface free energy, low dielectric constants, flame-retardancy, and excellent thermal and mechanical properties. This short review article describes the chemical and physical approaches that are used to prepare PBZs incorporating silica and carbon nanocomposites. In addition, recent reports of their physical properties are discussed, covering their dielectric constants and dynamic mechanical, thermal, electrical, and surface properties.

1. Introduction

Benzoxazine (BZ) monomers are heterocyclic compounds containing one oxygen and one nitrogen atom in a six-membered ring. They are synthesized through facile Mannich reactions from aromatic phenols, primary aliphatic or aromatic amines, and paraformaldehyde or formaldehyde solutions, within a solvent. Polybenzoxazines (PBZs) form a new class of thermosetting phenolic resins that can be prepared through thermal curing polymerization of various BZ monomers, without using a catalyst and without releasing byproducts (**Figure 1**).[1–8] PBZs can possess many attractive features including a high carbon residue, low surface energy, low moisture absorption, good thermal and mechanical properties, excellent dimensional stability, a stable dielectric constant, excellent flame retardancy, and good electrical properties that are not found for other traditional phenolic resins (e.g., phenolic bismaleimides, advanced epoxies).[9–20] Nevertheless, PBZs have limited applications at high temperature, because their C—N—C bonds break readily at temperatures above 260 °C.[21] As a result, many strategies have been tested to enhance the performance of PBZs. For example, i) introducing allyl and alkynyl groups into the BZ monomers, such that they can be polymerized to give products possessing 3D network structures; the resulting materials can display high moisture- and solvent-resistance and superior mechanical and thermal properties; ii) blending PBZs with other polymers or inorganic materials to improve the thermal properties through decreased chain mobility and the formation of cross-linked network structures.[22–29a] The thermomechanical responses of polymer matrices can be enhanced by using fillers; the applications of such materials as thermosetting phenolic resins strongly depends on the glass-transition temperature (T_g). Recently, Lazzaroni et al. studied, through molecular modeling, the influence of carbon nanotubes (CNTs) on the thermomechanical stability of two PBZ resins, P-pPDA and 4EP-pPDA, based on phenol-*p*-phenylene diamine and 4-ethylphenol-*p*-phenylene diamine. They found that these two PBZ nanocomposites responded differently, in terms of their values of T_g, to the presence of CNTs in the network.[29b] In 2018, Muthukaruppan et al. observed enhanced values of T_g, thermal stability, and char yield, and a lower thermal curing polymerization temperature, for ternary blends prepared from cardanol-BZ, traditional BZ, and bismaleimides. In addition, these BZ blends reinforced with a biosilica, derived from rice-husk ash functionalized with a silane derivative, exhibited lower dielectric constants.[29c] Such PBZ nanocomposites have potential uses as conducting coatings, mold releasing agents, packaging, green flame-retardants, and microelectronic fabrication devices. In this review, we focus on the methods of preparation of PBZs with two different types of inorganic materials (silicon- and carbon-based nanomaterials) to form PBZ nanocomposites, namely 1) PBZ/silica nanocomposites incorporating polydimethylsiloxane (PDMS), clays/layered silicates, and polyhedral oligomeric silsesquioxanes (POSS), and 2) PBZ/carbon nanocomposites incorporating carbon black, carbon fibers, CNTs, and graphene. We also discuss their resulting physical properties, including dielectric constants and dynamic mechanical, thermal, electrical, and surface properties.

2. PBZ/Silica Nanocomposites

Chemical and physical approaches have both been used to incorporate inorganic silica molecules into organic polymers.[30–33] The chemical approach can be more efficient than

Dr. M. G. Mohamed, Prof. S. W. Kuo
Department of Materials and Optoelectronic Science
Center for Functional Polymers and Supramolecular Materials
National Sun Yat-Sen University, Kaohsiung 80424, Taiwan
E-mail: kuosw@faculty.nsysu.edu.tw
The ORCID identification number(s) for the author(s) of this article can be found under https://doi.org/10.1002/macp.201800306.

DOI: 10.1002/macp.201800306

© 2018 WILEY-VCH Verlag GmbH & Co. KGaA, Weinheim

the physical approach, because of the formation of noncovalent or covalent bonds between the inorganic silica species and the polymer matrix can overcome macroscopic phase separation in the composite systems.

2.1. PBZ/PDMS Nanocomposites

PDMS is an elastomeric polymer that is composed of flexible and soft chains of polymers and crosslinking points.[34–36] Attaching PDMS to PBZs can improve the latter's thermal and mechanical properties, including its flexibility.[37,38] Because of the incompatibility of PDMS with PBZ thermosetting resins, modification of PDMS is necessary when introducing PDMS into PBZ resins.[39] Takeichi and co-workers[40] synthesized a high-molecular-weight PBZ containing PDMS units through condensation of α,ω-bis(aminopropyl)polydimethylsiloxane, bisphenol A, and formaldehyde to afford a B-PDMS BZ precursor. The resulting thermosets formed brown-colored transparent films after thermal curing at 240 °C; the elongation break increased upon increasing the molecular weight of PDMS, and the systems displayed high glass transition temperatures (T_g = 238–270 °C) and high thermal stability. In addition, Takeichi and co-workers also prepared three kinds of PBZ/polysiloxane hybrids through ring-opening polymerization of the BZ monomer PBa and subsequent hybridization of PBZ with PDMS, polymethylphenylsiloxane (PMPS), and polydiphenylsiloxane (PDPS). Based on dynamic viscoelastic analysis, PBa-PDMS exhibited two glass transition temperatures, whereas PBa-PMPS and PBa-PDPS exhibited only one value of T_g.[41] Chang et al. prepared a siloxane/imide-containing BZ monomer precursor through Mannich condensation of A6-OH with aniline and paraformaldehyde to afford BZ-A6 (**Figure 2**). The polymer derived from BZ-A6 exhibited, after a long period of thermal curing, a higher shear storage modulus, and a higher value of T_g (186 °C) than those of PBa (3.2 GPa and 174 °C, respectively), due to the former's greater crosslinking density, as determined through dynamic mechanical analysis (DMA). In addition, Chang et al. found that BZ-A6 formed a flexible film with low surface free energy and UV-resistance.[42] Alagar et al.[43] synthesized four allyl-terminated BZs through Mannich reactions of aromatic and aliphatic amines with 2-allylphenol and paraformaldehyde and then reacted these allyl BZ precursors with PDMS (through hydrosilylation in the presence of the catalyst Pt[dvs] in toluene) to obtain several PDMS-PBZ prepolymer hybrids (polydimethylsiloxane-diaminoethane-benzoxazine [PDMS-DAE-Bz], polydimethylsiloxane-diaminobutane-benzoxazine [PDMS-DAB-Bz], polydimethylsiloxane-diaminohexane-benzoxazine [PDMS-DAH-Bz]) (**Figure 3**). The contact angles of water and diiodomethane (DIM) of the PDMS-DAB-PBz and PDMS-DAH-PBz hybrids were higher than those of DAB-PBz and DAH-PBz, due the presence of weak dipole–dipole interactions in the layers of these systems. Furthermore, among these tested hybrids, the PDMS-DAH-PBz hybrid possessed the lowest dielectric constant of 2.42 MHz, presumably because of its long nonpolar aliphatic chains and superior layer-by-layer arrangement. In addition, Alagar and co-workers prepared BTMS/PDMS-PBz nanocomposites through thermal curing copolymerization of a BZ-terminated PDMS derivative (PDMS-PBz) with a BZ-terminated mesoporous MCM-41silica (BTMS).[44] We also synthesized a flexible and transparent DDSQ-BZ-PDMS copolymer through Mannich condensation of a bifunctional phenolic compound (DDSQ-BP), allyl amine, and formaldehyde (to afford a bis-allyl BZ DDSQ [DDSQ-BZ]) and subsequent hydrosilylation with PDMS (**Figure 4**A).[45] According to thermogravimetric analysis (TGA), the char yield of the thermally cured DDSQ-BZ-PDMS was 73 wt% and its degradation temperature (T_{d5}) was 335 °C; both values are higher than those of a traditional PBZ, due to the presence of the inorganic double decker silsesquioxane (DDSQ) cage and the increased crosslinking density after thermal curing polymerization. Furthermore, we found that the introduction of flexible PDMS could improve both the flexibility and transparency of DDSQ-BZ after thermally activated ring opening (Figures 4B,C).

Mohamed Gamal Mohamed received his B.Sc. in chemistry from Assiut University in 2004. Then, he received his M.Sc. in polymer chemistry at National Chiao Tung University under the supervision of Prof. Feng-Chih Chang. In 2016, he received his Ph.D. from the National Sun Yat-Sen University in polymer chemistry under the supervision of Prof. Shiao Wei Kuo. He is currently pursuing his postdoctoral works also at National Sun Yat-Sen University. His current research interests include polybenzoxazine, fluorescence polymers, AIE materials, and microporous conjugated polymers.

Shiao-Wei Kuo received his B.Sc. in chemical engineering from the National Chung Hsing University (1998) and Ph.D. in applied chemistry from the National Chiao Tung University in Taiwan (2002). He continued his research work at Chiao Tung University as a postdoctoral researcher during 2002–2007. Now, he is the professor in the Department of Materials and Optoelectronic Science, National Sun Yat-Sen University, Taiwan, and also the coordinator for polymer science program of minster of science and technology (MOST, Taiwan). His research interests include polymer interactions, self-assembly nanostructures, mesoporous materials, POSS nanocomposites, and polybenzoxazine, and polypeptides.

© 2018 WILEY-VCH Verlag GmbH & Co. KGaA, Weinheim

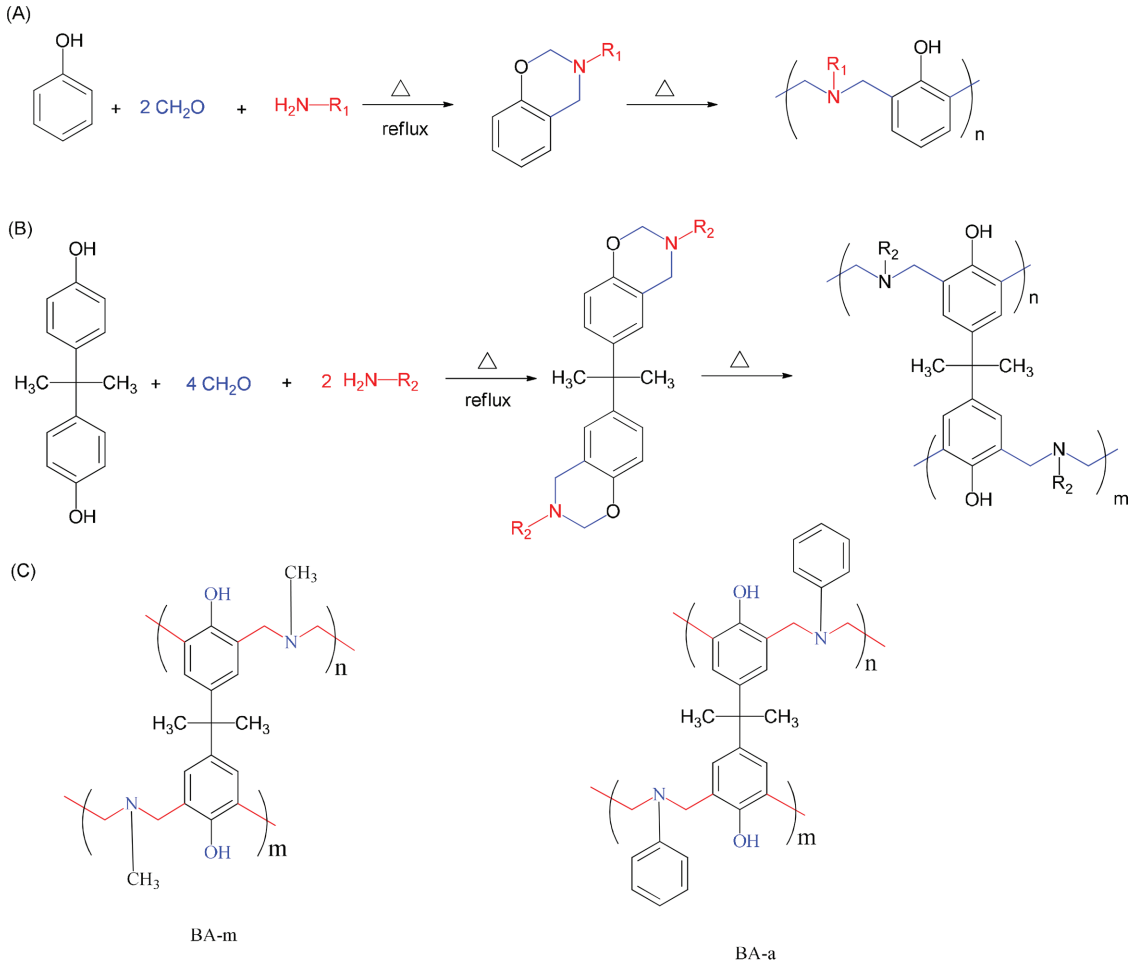

Figure 1. Preparation and thermally induced ring-opening polymerizations of A) P-a and B) B-a types of BZ monomers. C) Chemical structures of PBZs based on BA-m [2,2-bis(3,4-dihydro-3-methyl-2*H*-1,3-benzoxazin-6-yl)propane] and BA-a [2,2-bis(3,4-dihydro-3-phenyl-2*H*-1,3-benzoxazine)propane] BZ types of monomer.

2.2. PBZ/Clay or Layered Silicate Nanocomposites

Polymer/clay nanocomposites have been attractive materials for study because of their unique thermal properties, low combustion, and interesting optical properties.[46] There are two types of layered silicates: cationic and anionic. At present, the preparation of PBZ/clay nanocomposites remains challenging because of the low compatibility between BZ precursors and hydrophilic clays. Yagci et al.[47] synthesized PBZ/montmorillonite (PBz/MMT) nanocomposites through ion exchange of BPy^+ with the Na^+ ions in MTT, to afford an intercalated BZ clay (qBPy-MMT), and subsequent thermal curing polymerization with a fluid BZ monomer. Interestingly, using differential scanning calorimetry (DSC), the qBPy-MMT nanocomposites exhibited a broader exothermic curing peak at 303 °C, compared with those provided by Bpy and the quaternization of qBPy BZ monomers, due to the catalytic effect of the silicate layers accelerating the ring-opening polymerization of the BZ ring. Transmission electron microscopy (TEM) images of the PBZ/MMT nanocomposites revealed partially exfoliated/intercalated structures. We have also prepared new hybrid materials from cetylpyridinium chloride (CPC), clay, and poly(3-phenyl-3,4-dihydro-2*H*-1,3-benzoxazine) (PP-a).[48] These novel low-surface-free-energy materials, PBZ/organically modified silicate nanocomposites, possessed intercalated structures (based on X-ray analyses) as well as enhanced water contact angles, values of T_g and T_d, and char yields, compared with those of PP-a alone, when the clay loading was increased from 3 to 10 wt%. Gnanasundaram et al.[49] prepared PBZ/organoclay nanocomposites through a solvent-based method from PBZ resins and an organoclay (OMMT). Using X-ray diffraction, they found that the *d*-spacing of the OMMT interlayers increased from 1.69 to 2.10 nm after its dispersion within the PBZ precursors. We have also successfully introduced exfoliated MMT, by using POSS as the cationic surface, into PBZ, as displayed in **Figure 5**. Here, the thermal stability, surface hydrophobicity, mechanical properties, and values of T_g of the PBZ were enhanced/improved after incorporation of the exfoliated MMT.[50]

2.3. PBZ/POSS Nanocomposites

The chemistry of silsesquioxanes has become a hot topic in academia and industry because of their nano-sized stable 3D structures, composed of Si—O bonds in a cage structure with silicon

© 2018 WILEY-VCH Verlag GmbH & Co. KGaA, Weinheim

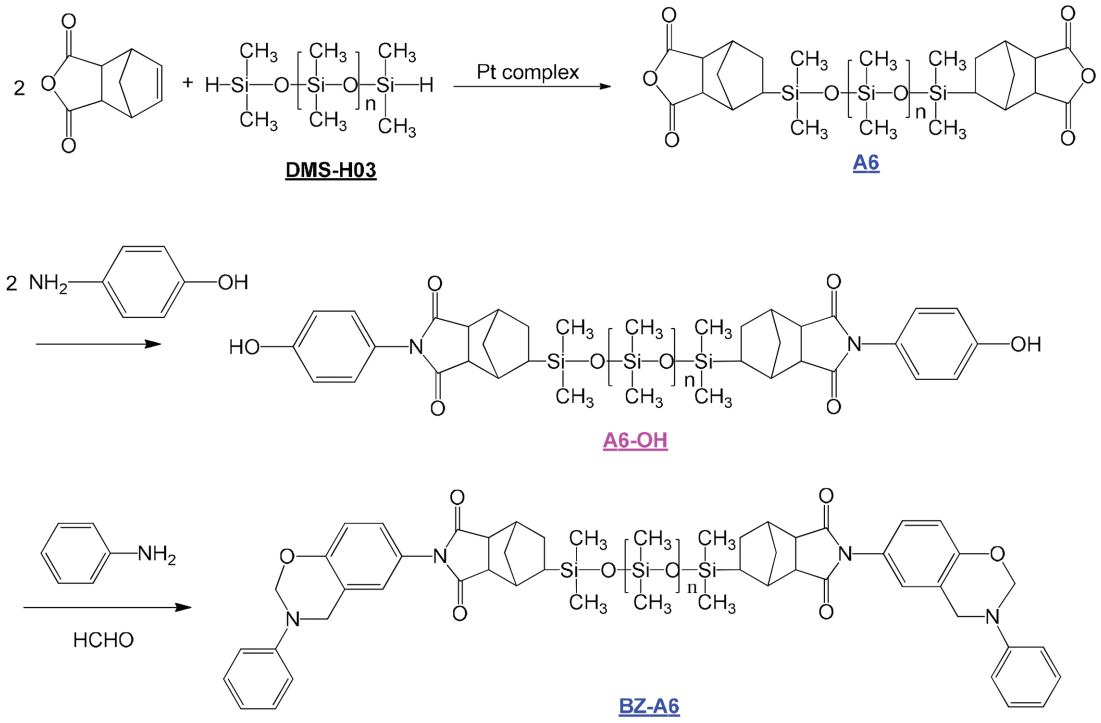

Figure 2. Synthesis of the BZ monomers A6-OH and BZ-A6. Reproduced with permission.[42] Copyright 2011, John Wiley and Sons.

atoms at the vertices. Silsesquioxanes have the chemical structure $(RSiO_{1.5})_n$, where R is the vertex group (e.g., hydrogen, alkyl, alkene, arylene) of the polyhedral molecule.[51–54] There are two kinds of molecular architectures for a silsesquioxane: a non-caged structure (including partial-cage, ladder, and random structures) and a cage-like structure (i.e., POSS). POSS molecules possess a highly symmetric T_8 cubic inorganic core having the chemical structure $R_8Si_8O_{12}$, with nanoscopic dimensions (diameters) ranging from 1 to 3 nm.[55–58] The introduction of POSS units into polymeric materials can decrease their heat evolution, flammability, and viscosity during processing and enhance their thermal and mechanical properties (e.g., rigidity, strength, modulus).[59–63] We have used two different strategies to prepare mono-functionalized BZ ring–containing hybrid organic/inorganic (POSS) materials (**Figure 6**)[64]: hydrosilylation of vinyl-terminated BZ with POSS (to obtain BZ-POSS-1) and Mannich condensation of a primary amine–containing POSS, phenol, and formaldehyde (to afford BZ-POSS-2). Their thermally activated ring-opening polymerizations with 3-phenyl-3,4-dihydro-2*H*-benzoxazine (Pa) and 6,6′-(propane-2,2-diyl)bis(3-phenyl-3,4-dihydro-2*H*-benzoxazine) (Ba) BZ monomers afforded Pa-POSS and Ba-POSS copolymer nanocomposites, respectively. The values of T_g and T_d and the char yields of the Pa-POSS and Ba-POSS copolymers

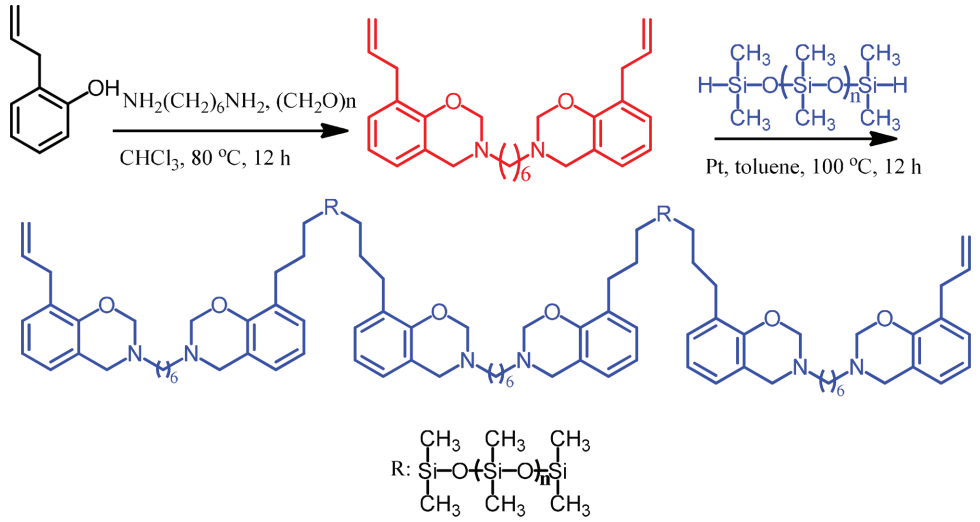

Figure 3. Schematic representation of the PDMS-Bz prepolymer. Reproduced with permission.[43] Copyright 2015, The Royal Society of Chemistry.

© 2018 WILEY-VCH Verlag GmbH & Co. KGaA, Weinheim

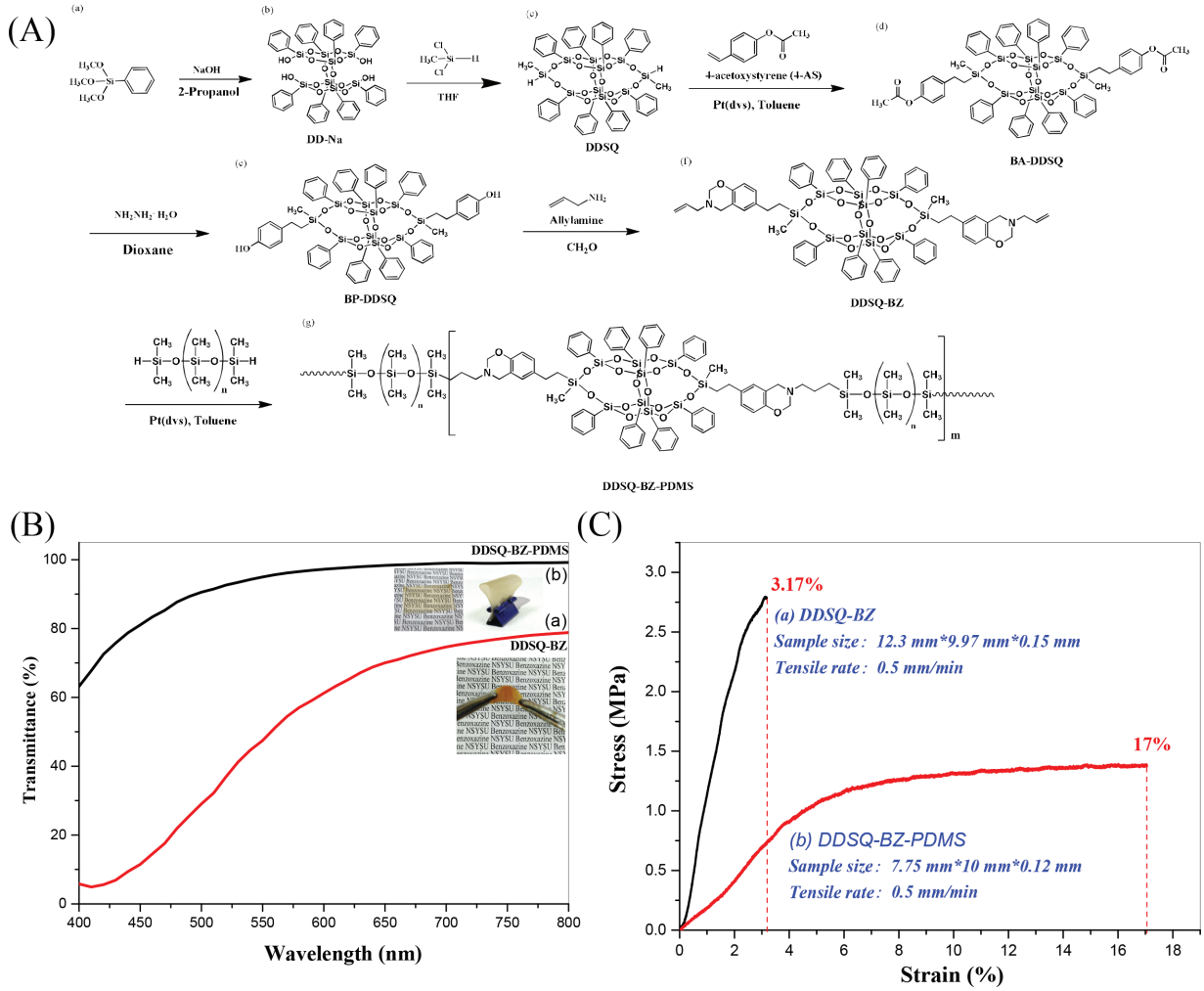

Figure 4. A) Synthesis of the prepolymer DDSQ-BZ-PDMS. B) UV spectra and C) stress–strain plots of DDSQ-BZ and DDSQ-BZ-PDMS after thermal curing. Reproduced with permission.[45] Copyright 2017, American Chemical Society.

increased upon increasing the content of the BZ-POSS derivatives from 0 to 10 wt%, suggesting that the POSS nanostructures restricted the mobility of the polymer chains. We have also prepared a multifunctional BZ–containing POSS derivative through the click reaction of an octaazido-functionalized POSS (OVPN3-POSS) and 3,4-dihydro-3-(prop-2-ynyl)-2*H*-benzoxazine (P-Pa).[65] The incorporation of rigid POSS units can lead to the formation of an inorganic protective layer on the surface of the resulting nanocomposite. Thus, this OBZ-POSS displayed a higher value of T_g and a higher char yield than those of P-pa and BA-m, respectively. Muthusamy et al.[66] synthesized three kinds of PBZ-tethered POSS derivatives through Mannich reactions of the bio-phenols eugenol (E), guaiacol (G), and vanillin (V) with octa(aminophenyl)silsesquioxane and formaldehyde to afford POSS-EBzo, POSS-GBzo, and POSS-VBzo, respectively. They used DMA to investigate the viscoelastic properties of these three POSS-PBZ nanocomposites. The values of G' for POSS-EBzo, POSS-GBzo, and POSS-VBzo were 2.63, 2.91, and 2.84 GPa, respectively. The enhancement of their dynamic properties, compared with those of eugenol-based PBZ,[67] may have been due to the presence of the POSS units covalently linked to the BZ moiety. Furthermore, the values of T_g for POSS-EBzo, POSS-GBzo, and POSS-VBzo were 118, 126, and 123 °C, respectively. We have prepared octuply adenine (A)–functionalized POSS (OBA-POSS) nanoparticles through reaction of adenine with OVBC-POSS.[68] OBA-POSS formed complementary hydrogen bonds with PA-T (T: thymine), as displayed in **Figure 7**A. The TEM patterns of PA-T and PA-T/OBA-POSS nanocomposites revealed (Figure 7B) that they self-assembled into long-range-ordered lamellar structures when the content of OBA-POSS was 10 or 20 wt%. Han and co-workers[69] prepared PBZ/POSS nanocomposites through the blending of a benzoxazole-modified $[PhSiO_{1.5}]_8$Bz monomer with BA-a. They used TGA to investigate the thermal stability of their PBZ/POSS nanocomposites. The decomposition temperature of the PBZ/POSS nanocomposites increased from 306 to 434 °C upon increasing the content of OPS-BZ, due to the presence of the inorganic cage (POSS) units and the formation of crosslinked network structures. In addition, the dielectric constant of the PBZ/POSS nanocomposites improved upon increasing the content of OPS-BZ under a low frequency of 1 MHz. In contrast, increasing the content of POSS in the

© 2018 WILEY-VCH Verlag GmbH & Co. KGaA, Weinheim

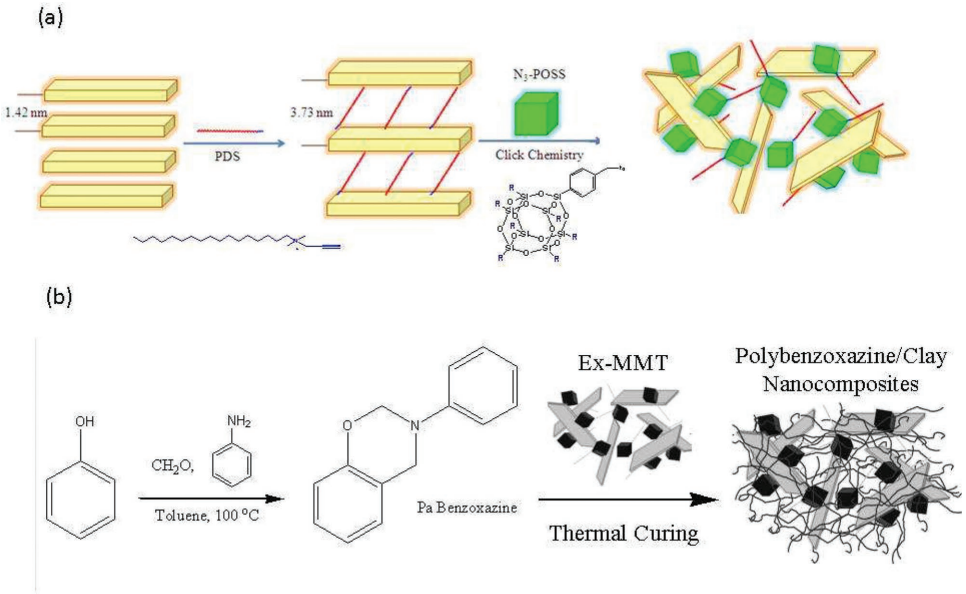

Figure 5. Preparation of a) exfoliated MMT through a click reaction and b) PBZ/clay nanocomposites. Reproduced with permission.[50] Copyright 2013, Springer.

PBZ/POSS nanocomposites caused the dielectric constant of the PBZ/POSS nanocomposites to decrease. Zheng et al.[70] synthesized DDSQ-PBZ copolymers incorporating a double-decker silsesquioxane in the main chain (**Figure 8**). These organic/inorganic copolymers exhibited excellent film forming properties and high molecular weights. In addition, based on static contact angle measurements, these organic/inorganic DDSQ-PBZ copolymers displayed improved surface hydrophobicity after increasing the weight ratio of DDSQ.

3. PBZ/Carbon Nanocomposites

Relatively new carbon materials, including graphene, CNTs, and fullerenes (C_{60}), have attracted much academic and industrial attention because of their unique and interesting chemical, optoelectronic, and physical properties.[71–74] Herein, we discuss the preparation and properties of PBZ/carbon nanocomposites incorporating carbon fibers, carbon black, CNTs, and graphene.

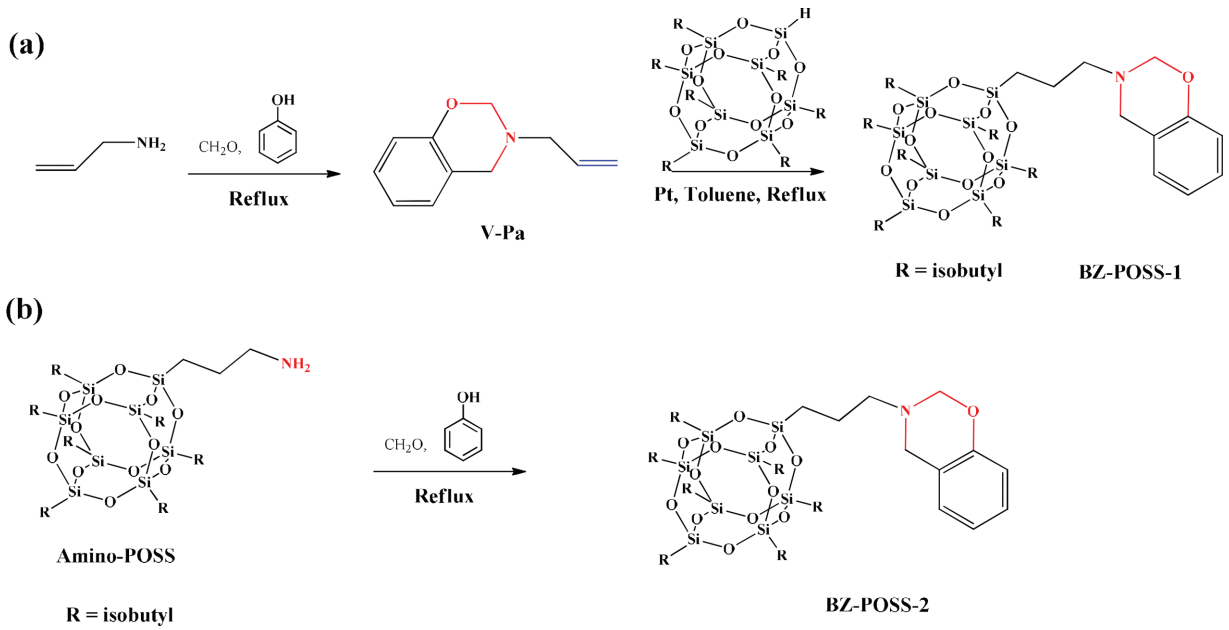

Figure 6. Synthesis of a) the VP-a monomer and b) BZ-POSS-2 from amino-POSS. Reproduced with permission.[64] Copyright 2004, Elsevier.

© 2018 WILEY-VCH Verlag GmbH & Co. KGaA, Weinheim

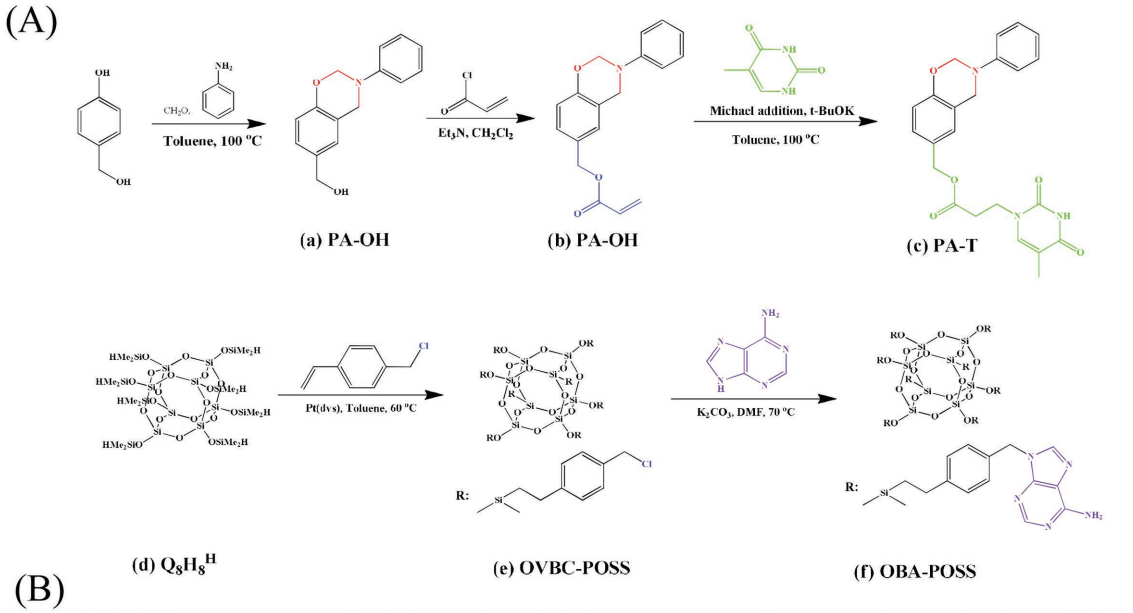

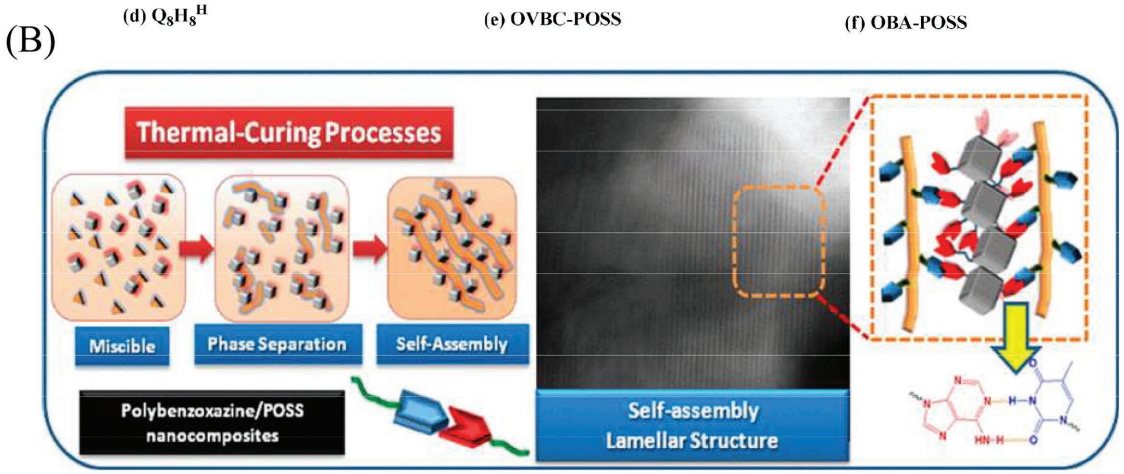

Figure 7. A) Synthesis of PA-T and OBA-POSS. B) TEM images and possible formation of complementary hydrogen bonds between OBA-POSS and PA-T (T: thymine) in their nanocomposites. Reproduced with permission.[68] Copyright 2012, American Chemical Society.

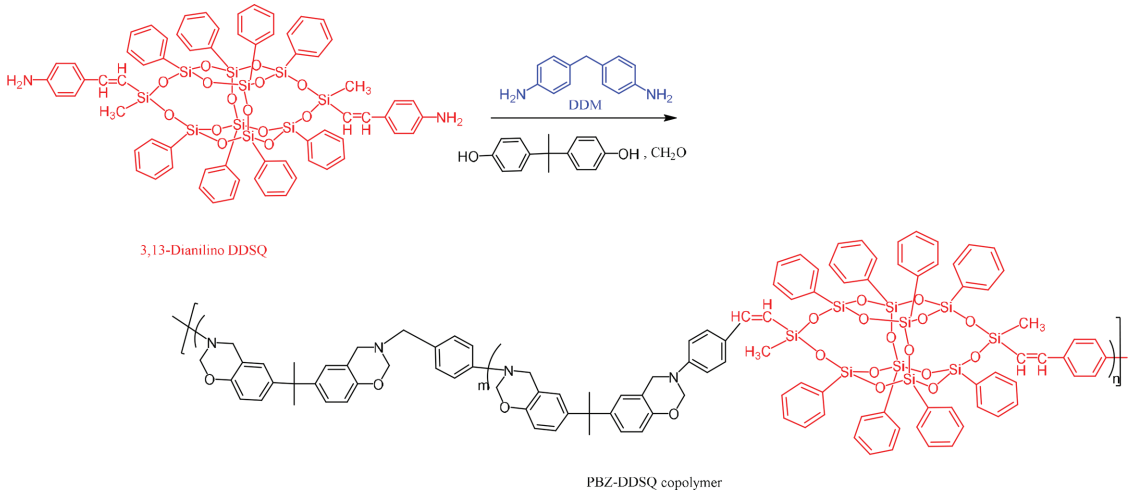

Figure 8. Synthesis of organic/inorganic main-chain PBZ-DDSQ copolymers. Reproduced with permission.[70] Copyright 2007, Elsevier.

© 2018 WILEY-VCH Verlag GmbH & Co. KGaA, Weinheim

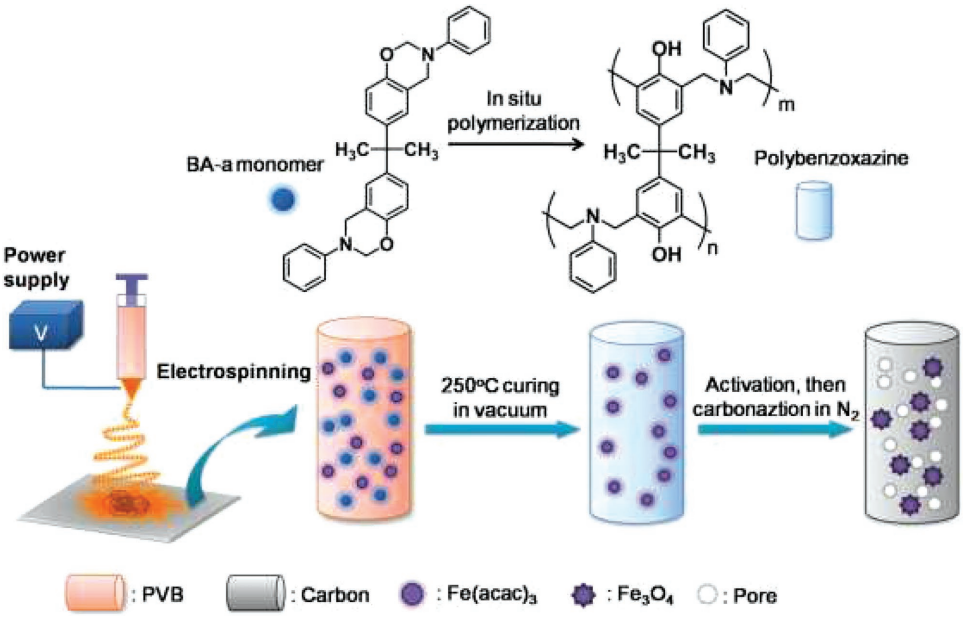

Figure 9. Schematic representation of the preparation of A-FeCNF. Reproduced with permission.[77] Copyright 2012, Elsevier.

3.1. PBZ/Carbon Fiber or Carbon Black Nanocomposites

Carbon nanofibers (CNFs) are 1D nanostructured materials of great scientific and technological interest because of their high temperature-resistance, large specific surface areas, and excellent electrical and thermal conductivities.[75,76] Ding et al.[77] prepared hierarchical porous and magnetic Fe_3O_4@carbon fibers based on PBZ through a combination of electrospinning, in situ polymerization of BZ precursors, and an activation process to obtain magnetic A-Fe@CNF (**Figure 9**). They found that the resultant A-Fe@CNF species had an average diameter of 130 nm and a high surface area (1885 $m^2\ g^{-1}$). In addition, the magnetic A-Fe@CNF was highly applicable for the adsorption of organic dyes in water. Ding et al. also prepared hierarchical porous, magnetic Fe_3O_4@carbon nanofibers (Fe_3O_4@CNFs) through electrospinning of polyacrylonitrile/PBZ nanofibers and an activation process.[78] According to Brunauer–Emmett–Teller measurements, a series of Fe_3O_4@CNFs with tunable micro- and mesoporous structure had high surface areas (up to 1623 $m^2\ g^{-1}$). Furthermore, the as-prepared Fe_3O_4@CNFs adsorbed organic dyes efficiently in water and had excellent magnetic separation performance, as displayed in **Figure 10**. Alagar et al.[79] prepared PBZ nanocomposites reinforced with functionalized carbon black (FCB) through thermal curing polymerization of a BZ precursor with various contents of FCB. They found that the dielectric constant and electrical conductivity both improved after incorporation of the FCB.

3.2. PBZ/CNT Nanocomposites

CNTs are hollow cylinders, composed of single or multiple sheets that can be several micrometers in length and a few nanometers in diameter. There are two kinds of CNTs: single-walled CNTs (SWCNTs) and multi-walled CNTs (MWCNTs), characterized by the number of graphene layers forming the walls. A SWCNT consists of a single layer of graphene wrapped to a diameter of 1 nm; MWCNTs feature multiple layers of graphene and have diameters ranging from 2 to 100 nm.[80–82] CNTs exhibit unique thermal, electrical, and mechanical properties.[83–85] There have been two approaches developed to improve the homogeneous dispersion and deaggregation of CNTs within a polymer matrix: covalent bonding (through modification and functionalization of the CNT's walls)[86,87] and physical bonding (through physical interactions, including van der Waals and π–π interactions, of organic molecules [e.g., pyrene] with the CNT's walls, without altering the hybridization of the carbon atoms (e.g., from sp^2 to sp^3) at the CNT's surface).[88–91] These two approaches have been applied to incorporate CNTs within PBZ matrices. We have reported three examples concerning the π-stacking interactions of PBZs presenting pyrene units and CNT walls. For example, we synthesized a pyrene-functionalized BZ monomer (Py-BZ; **Figure 11**A) and blended it with SWCNTs to obtain Py-BZ/SWCNT hybrid complexes stabilized through noncovalent bonding. A subsequent thermally activated ring-opening polymerization, without a catalyst, afforded poly(Py-BZ)/SWCNT nanocomposites (Figure 11B). Interestingly, DSC analysis of Py-BZ systems with various SCWNT contents revealed that the maximum exothermic curing peak of the Py-BZ/SWNCTs (238 °C) was lower than that of the pure Py-BZ (286 °C) because of a catalytic effect of the SWCNTs (Figure 11C). In addition, high-resolution TEM images (Figure 11D) revealed a uniform and excellent dispersion of the SWCNTs within the polymer (Py-BZ) matrix, without any aggregation.[92] More interestingly, we have prepared a multifunctional BZ monomer, coumarin-PyBz, containing coumarin units (as photoresponsive sites) and pyrene units (for π-stacking), through a facile Mannich condensation of 4-methyl-7-hydroxycoumarin, paraformaldehyde, and

© 2018 WILEY-VCH Verlag GmbH & Co. KGaA, Weinheim

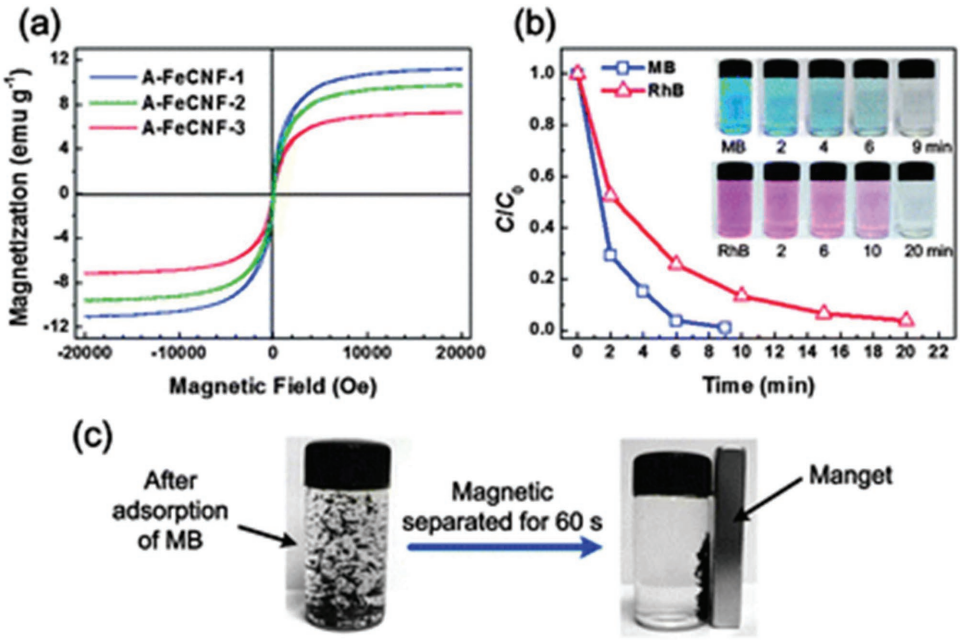

Figure 10. a) Magnetic hysteresis loops of A-FeCNF-1, A-FeCNF-2, and A-FeCNF-3. b) Plots of C/C_0 with respect to time for adsorption of dye solutions onto A-FeCNF-3. c) Photograph of the magnetic responsive performance of A-FeCNF-3 after adsorption of MB (9 min). Reproduced with permission.[78] Copyright 2012, The Royal Society of Chemistry.

1-aminopyrene, and performed photodimerization (through [2π–2π] cycloaddition) of its coumarin units under UV irradiation at 365 nm to obtain di(coumarin-PyBz).[93] We then prepared poly(coumarin-PyBz) and poly(dicoumarin-PyBZ)/SWCNT hybrid nanocomposites by exploiting noncovalent interactions and thermally activated ring-opening polymerization. Photoluminescence (PL) measurements revealed that the emission band of coumarin-PyBz at 430 nm was quenched

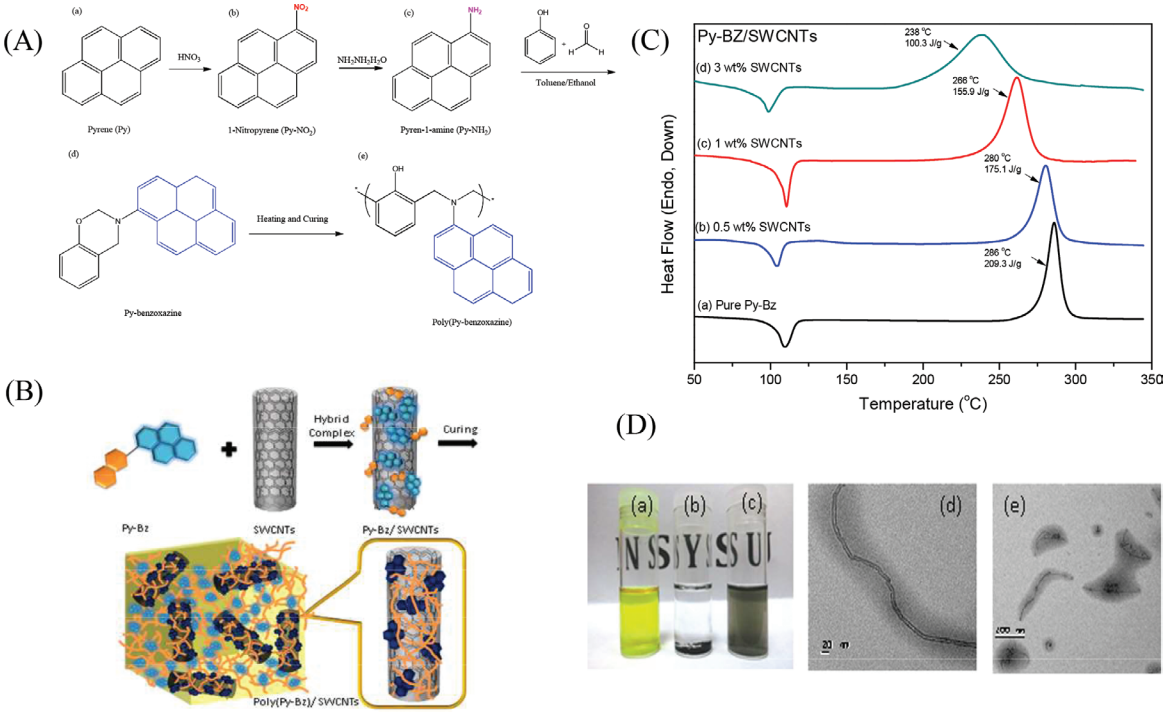

Figure 11. A) Schematic representation of poly(Py-benzoxazine). B) Cartoon representation of the preparation of Py-BZ/SWCNT and poly(Py-BZ)/SWCNT nanocomposites through physical interactions. C) DSC thermograms of the curing behavior of Py-BZ at SWCNT contents from 0.5 to 3 wt%. D) TEM image of the thermally cured Py-BZ/SWCNT composite. Reproduced with permission.[92]Copyright 2014, Elsevier.

© 2018 WILEY-VCH Verlag GmbH & Co. KGaA, Weinheim

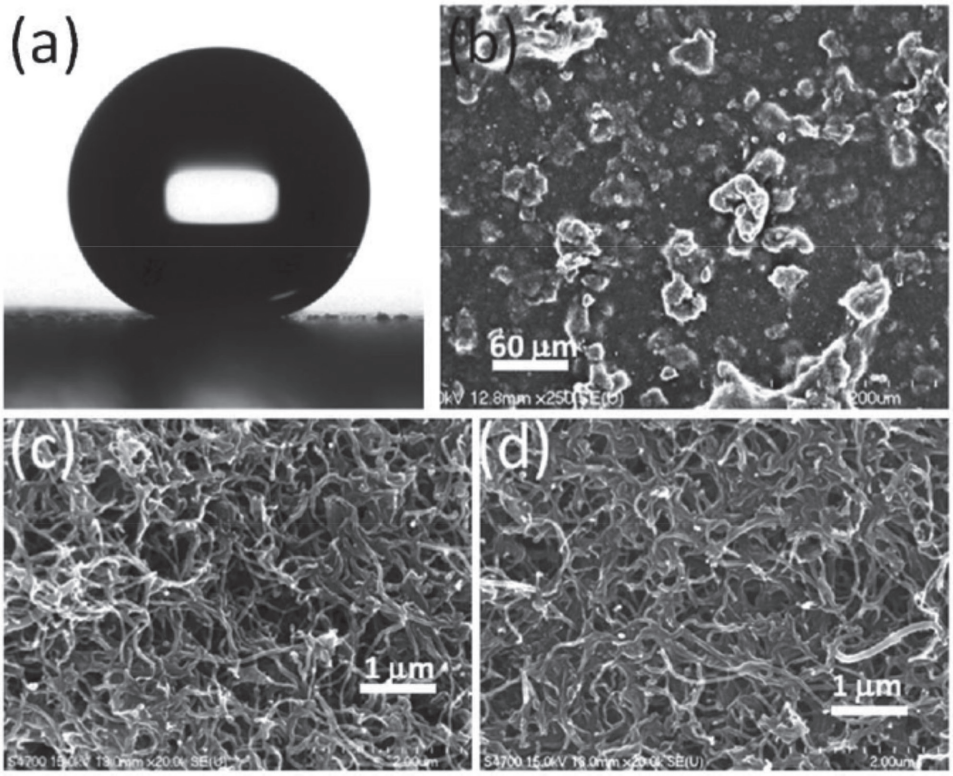

Figure 12. a) Profile of a water drop on the m-MWCNT-PBZ surface. b–d) SEM images of the superhydrophobic surface of m-MWCNT-PBZ. Reproduced with permission.[95] Copyright 2013, The Royal Society of Chemistry.

after its blending with the SWCNTs, suggesting the presence of strong π-stacking interactions between the pyrene units and the SWCNTs. This PBZ/SWCNT hybrid nanocomposite formed a homogeneous dispersion, without any aggregation, and featured less-entangled SWCNTs within the PBZ matrix, as revealed through TEM imaging. Based on DSC analysis, the glass transition temperatures of poly(coumarin-Py BZ), poly(dicoumarin Py BZ), poly(coumarin-Py BZ)/3 wt% SWCNT, and poly(dicoumarin-Py BZ)/3 wt% SWCNT were 200, 227, 185, and 205 °C, respectively. The value of T_g of poly(dicoumarin-Py BZ)/3 wt% SWCNT (205 °C) was higher than that of poly(coumarin-Py BZ)/SWCNT (3 wt%) because photodimerization of the coumarin units increased the crosslinking density. TGA analysis revealed that, without UV irradiation, the poly(dicoumarin Py BZ)/SWCNT (3 wt%) nanocomposite had a higher decomposition temperature and char yield than those of the coumarin-containing PBZ, presumably because of the effect of the increased crosslinking density and nano-reinforcement. We also prepared a trifunctional Azo-COOH-PyBz monomer through condensation of Azo-COOH, 1-aminopyrene (pyrene-NH_2), and paraformaldehyde.[94] Because Azo-COOH-PyBz contained a pyrene unit, it improved the dispersion of CNTs through π-stacking; because of the presence of the carboxyl group and the catalytic effect of the SWCNTs, the maximum exothermic curing peak for the Azo-COOH-PyBz/SWCNT hybrid complexes shifted to lower temperature, compared with that of poly(Azo-COOH-PyBz), based on DSC thermograms. TGA analysis was used to investigate the effect of SWCNTs and MWCNTs on the thermal stability of Azo-COOH-PyBz after thermal curing polymerization; it revealed that the char yield and value of T_d of poly(Azo-COOH-PyBz) increased to greater degrees in the presence of SWCNTs than in the presence of MWCNTs, possibly because of the greater thermal conductivity of the SWCNTs within the PBZ matrix. Yang et al.[95] prepared superhydrophobic PBZ/MWCNT nanocomposites through microwave irradiation at 2.45 GHz. They used SEM to investigate the morphology of the m-MWCNT/PBZ nanocomposites. These rough substrates possessed micro- and nanoscale binary structures (**Figure 12**). Furthermore, the water contact angle of the MWCNT/BZ nanocomposite decreased from 160 to 137° within 30 min of preparation; in contrast, water droplets on the m-MWCNT/PBZ surface remained near-spherical after 30 min, indicating a stable superhydrophobicity for this system. Doubis et al.[96] prepared two BZ monomers, BPA-BZ and MDF-Bz, through Mannich condensations, and then blended them with various contents of MWCNTs to afford PBZ/MWCNT nanocomposites. For both monomers, the single exothermic curing temperature (255 °C for BPA-BZ; 265 °C for MDF-Bz) shifted to a slightly lower temperature in the presence of the MWCNTs, due to the improved thermal conductivity and suppressed polymerization heat of each system.

3.3. PBZ/Graphene Nanocomposites

Graphene is a single-atom-thick 2D carbon material displaying high thermal resistance, high Young's modulus, and good excellent fracture strength.[97] Graphene oxide (GO) is a layered,

© 2018 WILEY-VCH Verlag GmbH & Co. KGaA, Weinheim

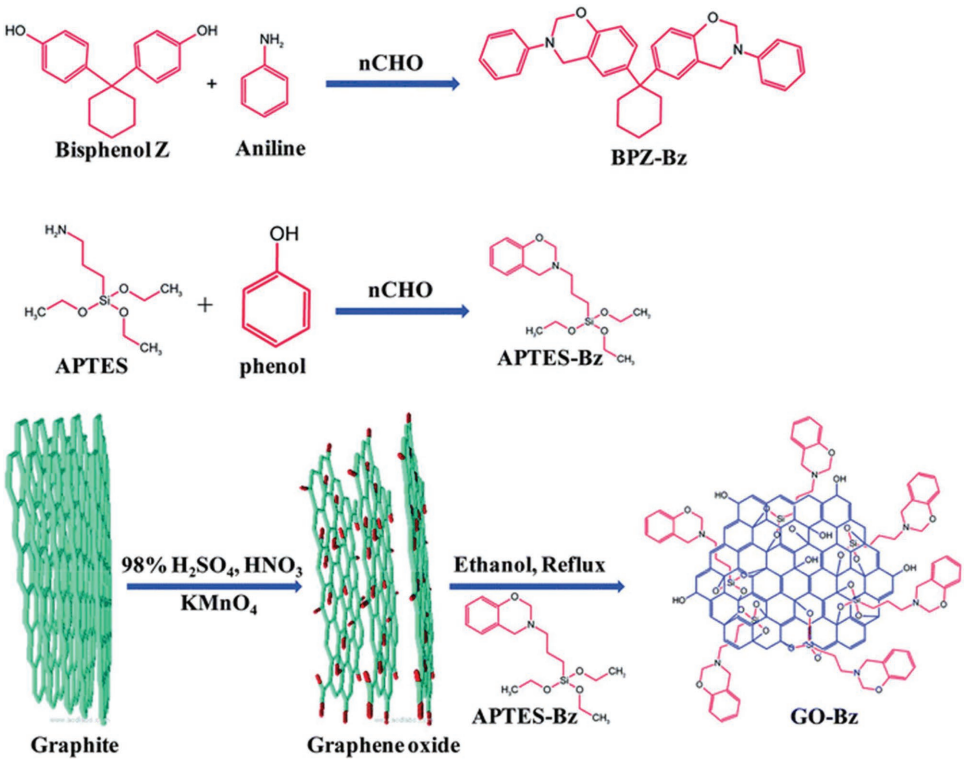

Figure 13. Preparation of the BZ monomer, APTES-BZ, and GO-BZ materials. Reproduced with permission.[100] Copyright 2015, The Royal Society of Chemistry.

atomically thin sheet that is highly functionalized with several oxygen atoms (e.g., OH and COOH groups) on its surface. GO can be prepared through oxidation of graphite.[98] The incorporation of GO within a PBZ matrix can improve the performance over that of neat PBZ. Ishida et al.[99] prepared the BZ monomer SLTB(4HBA-T403) through Mannich condensation of 4-hydroxbenzaldehyde with paraformaldehyde and jeffamine T-403. GO was then reinforced into the PBZ precursor, through freeze-drying of a GO suspension, to afford GO-reinforced PBZ nanocomposite aerogels. SEM was used to investigate the morphologies and microstructures of the GO-reinforced PBZ aerogels and the neat PBZ in the absence of GO. The number of layers and the porosity both increased upon increasing the GO content. Alagar et al.[100] lowered the dielectric constant of bisphenol-Z PBZ through reinforcement of GO within a BPZ-PBz matrix (**Figure 13**). The 10 wt% GO/BPZ-PBz nanocomposite exhibited the lowest dielectric constant (1.95) among their tested GO-BPZ-PBz nanocomposites. Yan et al. synthesized PBZ/carboxylated-GO (GO-COOH) hybrid nanocomposites through in situ intercalative polymerization. They found that the presence of 1 wt% of GO-COOH improved the thermal stability and increased the value of T_g of GO-COOH/BOZ, compared with those of the pure PBZ.[101]

4. Conclusions

The use of inorganic/organic hybrid materials containing silicon- and carbon-based materials as nanocomposites within PBZ precursors has remained an active topic in both academic and industrial research because it can enhance the performance of PBZ and improve its properties. In addition, these materials have many potential applications, for example, in conductive coatings, mold releasing agents, packaging, green flame-retardants, low-*k* adhesives, and microelectronic fabrication devices.

Acknowledgements

M.G.M. and S.-W.K. both contributed to the literature review and to the writing of this paper. This study was supported financially by the Ministry of Science and Technology, Taiwan, under contracts MOST 106-2221-E-110-067-MY3 and 105-2221-E-110-092-MY3.

Conflict of Interest

The authors declare no conflict of interest.

Keywords

benzoxazine monomers, double decker silsesquioxanes, layered silicates, polybenzoxazines, polydimethylsiloxanes, polyhedral oligomeric silsesquioxanes, thermal curing polymerizations

Received: July 18, 2018
Revised: October 15, 2018
Published online:

[1] L. Lin, T. Agag, Y. Yagci, H. Ishida, *Macromolecules* **2011**, *44*, 767.
[2] T. Endo, A. Sudo, *J. Polym. Sci., Part A: Polym. Chem.* **2009**, *47*, 4847.

© 2018 WILEY-VCH Verlag GmbH & Co. KGaA, Weinheim

[3] T. Agag, C. R. Arza, F. H. J. Maurer, H. Ishida, *Macromolecules* **2010**, *43*, 2748.
[4] C. F. Wang, S. F. Chiou, F. H. Ko, J. K. Chen, C. T. Chou, C. F. Huang, S. W. Kuo, F. C. Chang, *Langmuir* **2007**, *23*, 5868.
[5] C. P. R. Nair, *Prog. Polym. Sci.* **2004**, *29*, 401.
[6] X. Ning, H. Ishida, *J. Polym. Sci., Part A: Polym. Chem.* **1994**, *32*, 1121.
[7] N. N. Ghosh, B. Kiskan, Y. Yagci, *Prog. Polym. Sci.* **2007**, *32*, 1344.
[8] a) F. Holly, A. C. Cope, *J. Am. Chem. Soc.* **1944**, *66*, 1875; b) J. Zhao, Muhammad R. H. S. Gilani, Z. Liu, R. Luque, G. Xu, *Polym. Chem* **2018**, *9*, 4324; c) S. R. Kumar, S. K. Mohanb, J. Dhanasekaran, *New J. Chem* **2018**, *42*, 16083.
[9] D. P. Sanders, H. Ishida, *Macromolecules* **2000**, *33*, 8149.
[10] C. F. Wang, H. Y. Chen, S. W. Kuo, Y. S. Lai, P. F. Yang, *RSC Adv.* **2013**, *3*, 9764.
[11] C. F. Wang, Y. C. Su, S. W. Kuo, C. F. Huang, Y. C. Sheen, F. C. Chang, *Angew. Chem., Int. Ed.* **2006**, *45*, 2248.
[12] H. Ishida, *Handbook of Polybenzoxazine Resins* (Eds: H. Ishida, T. Agag), Elsevier, Amsterdam, **2011**, Ch. 1, p. 1.
[13] T. Agag, T. Takeichi, *Macromolecules* **2003**, *36*, 6010.
[14] S. W. Kuo, W. C. Lin, *J. Appl. Polym. Sci.* **2010**, *117*, 3121.
[15] B. Kiskan, B. Aydon, Y. Yagci, *J. Polym. Sci., Part A: Polym. Chem.* **2009**, *47*, 804.
[16] C. F. Wang, T. F. Wang, C. S. Liao, S. W. Kuo, H. C. Lin, *J. Phys. Chem. C* **2011**, *115*, 16495.
[17] T. Agag, T. Takeichi, *Macromolecules* **2001**, *34*, 7257.
[18] A. Chernykh, T. Agag, H. Ishida, *Polymer* **2009**, *50*, 3153.
[19] J. M. Huang, S. W. Kuo, Y. J. Lee, F. C. Chang, *J. Polym. Sci., Part B: Polym. Phys.* **2007**, *45*, 644.
[20] R. C. Lin, M. G. Mohamed, S. W. Kuo, *Macromol. Rapid Commun.* **2017**, *38*, 1700251.
[21] H. Y. Low, H. Ishida, *J. Polym. Sci., Part B: Polym. Phys.* **1998**, *36*, 1935.
[22] Z. Brunovska, H. Ishida, *J. Appl. Polym. Sci.* **1999**, *73*, 2937.
[23] M. G. Mohamed, W. C. Su, Y. C. Lin, C. F. Wang, J. K. Chen, U. K. Jeong, S. W. Kuo, *RSC Adv.* **2014**, *4*, 50373.
[24] H. Oie, A. Sudo, T. Endo, *J. Polym. Sci., Part A: Polym. Chem.* **2013**, *51*, 2035.
[25] S. Ohashi, V. Pandey, R. Arza, P. Frimowicz, H. Ishida, *Polym. Chem.* **2016**, *7*, 2245.
[26] K. D. Demir, B. Kiskan, Y. Yagci, *Macromolecules* **2011**, *44*, 1801.
[27] B. Kiskan, N. N. Ghosh, Y. Yagci, *Polym. Int.* **2011**, *60*, 167.
[28] Y. H. Wang, C. M. Chang, Y. L. Liu, *Polymer* **2012**, *53*, 106.
[29] a) H. Ishida, J. D. Allen, *Polymer* **1996**, *37*, 4487; b) S. Saiev, L. Bonnaud, L. Dumas, T. Zhang, P. Dubois, D. Beljonne, R. Lazzaroni, *ACS Appl. Mater. Interfaces* **2018**, *10*, 26669; c) H. Arumugam, S. Krishnan, M. Chavali, A. Muthukaruppan, *New J. Chem.* **2018**, *42*, 4067; d) C. C. Tsai, Z. Gan, S. W. Kuo, *Polym. Chem.* **2018**, *9*, 3684.
[30] S. W. Kuo, F. C. Chang, *Prog. Polym. Sci.* **2011**, *36*, 1649.
[31] J. Wu, P. T. Mather, *Polym. Rev.* **2009**, *49*, 25.
[32] J. Choi, J. Harcup, A. F. Yee, Q. Zhu, R. M. Laine, *J. Am. Chem. Soc.* **2001**, *123*, 11420.
[33] A. Striolo, C. McCabe, P. T. Cummings, *J. Chem. Phys.* **2006**, *125*, 104904.
[34] H. Ardhyananta, T. Kawauchi, H. Ismail, T. Takeichi, *Polymer* **2009**, *50*, 5959.
[35] R. Taniguchi, T. Yamada, K. Sada, K. Kokado, *Macromolecules* **2014**, *47*, 6382.
[36] H. Ardhyananta, M. H. Wahid, M. Sasaki, T. Agag, T. Kawauchi, H. Ismail, T. Takeichi, *Polymer* **2008**, *49*, 4585.
[37] W. Li, J. Chu, L. Heng, T. Wei, J. Gu, K. Xi, X. Jia, *Polymer* **2013**, *54*, 4909.
[38] B. Aydogan, D. Sureka, B. Kiskan, Y. Yagci, *J. Polym. Sci., Part A: Polym. Chem.* **2010**, *48*, 5156.
[39] H. Ardyanata, T. Kawauchi, T. Takeichi, H. Ismail, *High Perform. Polym.* **2010**, *22*, 609.
[40] T. Takeichi, T. Kano, T. Agag, T. Kawauchi, N. Furukawa, *J. Polym. Sci., Part A: Polym. Chem.* **2001**, *39*, 2633.
[41] H. Ardhyananta, T. Kawauchi, H. Ismail, T. Takeichi, *Polymer* **2009**, *50*, 5959.
[42] K. C. Chen, H. T. Li, S. C. Huang, W. C. Chen, K. W. Sun, F. C. Chang, *Polym. Int.* **2011**, *60*, 1089.
[43] R. S. Kumar, N. Padmanathan, M. Alagar, *New J. Chem.* **2015**, *39*, 3995.
[44] R. S. Kumar, M. Ariraman, M. Alagar, *RSC Adv.* **2015**, *5*, 40798.
[45] Y. T. Liao, Y. C. Lin, S. W. Kuo, *Macromolecules* **2017**, *50*, 5739.
[46] S. S. Ray, M. Okamoto, *Prog. Polym. Sci.* **2003**, *28*, 1539.
[47] K. D. Demir, M. A. Tasdelen, T. Uyar, A. W. Kawaguchi, A. Studo, T. Endo, Y. Yagci, *J. Polym. Sci., Part A: Polym. Chem.* **2009**, *47*, 804.
[48] H. K. Fu, C. F. Huang, S. W. Kuo, H. C. Lin, D. Ru Yei, F. C. Chang, *Macromol. Rapid Commun.* **2008**, *29*, 1216.
[49] C. K. Chozhan, M. Alagar, P. Gnanasundaram, *Acta Mater.* **2009**, *57*, 782.
[50] H. W. Cui, S. W. Kuo, *J. Polym. Res.* **2013**, *20*, 114.
[51] a) D. B. Cordes, P. D. Lickiss, F. Rataboul, *Chem. Rev.* **2010**, *110*, 2081; b) M. G. Mohamed, K. C. Hsu, S. W. Kuo, *Polym. Chem.* **2016**, *7*, 135.
[52] D. W. Scott, *J. Am. Chem. Soc.* **1946**, *68*, 356.
[53] Q. Chen, R. Xu, J. Zhang, D. Yu, *Macromol. Rapid Commun.* **2005**, *26*, 1878.
[54] G. Li, L. Wang, H. Ni, C. U. Pittman Jr, *J. Inorg. Organomet. Polym.* **2001**, *11*, 123.
[55] H. Zhou, Q. Ye, J. Xu, *Mater. Chem. Front.* **2017**, *1*, 212.
[56] A. Sellinger, R. M. Laine, *Macromolecules* **1996**, *29*, 2327.
[57] M. Z. Asuncion, M. F. Roll, R. M. Laine, *Macromolecules* **2008**, *41*, 8047.
[58] J. Zhnag, R. Xu, D. S. Yu, *Eur. Polym. J.* **2007**, *43*, 743.
[59] C. M. Leu, Y. T. Chang, K. H. Wei, *Chem. Mater.* **2003**, *15*, 3721.
[60] J. C. Huang, C. B. He, X. Xiao, K. Y. Mya, J. Dai, Y. P. Siow, *Polymer* **2003**, *44*, 2739.
[61] C. M. Leu, T. Y. Chang, K. H. Wei, *Macromolecules* **2003**, *36*, 9122.
[62] A. Ebunoluwa, S. Biswajit, A. Paschalis, *Nanomaterials* **2012**, *2*, 445.
[63] A. Strachota, I. Kroutilova, J. Kovaro, L. Matejka, *Macromolecules* **2004**, *37*, 9457.
[64] Y. J. Lee, S. W. Kuo, Y. C. Su, J. K. Chen, C. W. Tu, F. C. Chang, *Polymer* **2004**, *45*, 6321.
[65] Y. C. Wu, S. W. Kuo, *Polymer* **2010**, *51*, 3948.
[66] T. Periyasamy, S. P. Asrafali, S. Muthusamy, *New J. Chem.* **2015**, *39*, 1691.
[67] P. Thirukumaran, A. S. Parveen, M. Sarojadevi, *RSC Adv.* **2014**, *4*, 7959.
[68] W. H. Hu, K. W. Huang, C. W. Chiou, S. W. Kuo, *Macromolecules* **2012**, *45*, 9020.
[69] K. Zhang, Q. Zhuang, X. Liu, G. Yang, R. Cai, Z. Han, *Macromolecules* **2013**, *46*, 2696.
[70] N. Liu, L. Li, L. Wang, S. Zhang, *Polymer* **2017**, *109*. 254.
[71] H. Zhu, J. Wei, K. Wang, D. Wu, *Sol. Energy Mater. Sol. Cells* **2009**, *93*, 1461.
[72] D. S. Su, G. Centi, *J. Energy Chem.* **2013**, *22*, 151.
[73] Y. He, W. Chen, C. Gao, J. Zhou, X. Li, E. Xie, *Nanoscale* **2013**, *5*, 8799.
[74] M. G. Mohamed, R. C. Lin, S. W. Kuo, *Advanced and Emerging Polybenzoxazine Science and Technology* (Eds: H. Ishida, P. Froimowicz), Elsevier, Amsterdam **2017**, Ch. 36 , p. 725.
[75] W. Zhang, Z. Y. Wu, H. L. Jiang, S. H. Yu, *J. Am. Chem. Soc.* **2014**, *136*, 14385.
[76] R. J. Warzoha, D. Zhang, G. Feng, A. S. Fleischer, *Carbon* **2013**, *61*, 441.

© 2018 WILEY-VCH Verlag GmbH & Co. KGaA, Weinheim

[77] Y. Si, T. Ren, Y. Li, B. Ding, J. Wu, *Carbon* **2012**, *50*, 5176.
[78] T. Ren, Y. Si, J. Yang, B. Ding, X. Yang, F. Hong and J. Yu, *J. Mater. Chem.* **2012**, *22*, 15919.
[79] M. Selvi, S. Devaraju, K. Sethuraman, M. Alagar, *Polym. Compos.* **2014**, *35*, 2121.
[80] J. L. Bahr, J. M. Tour, *J. Mater. Chem.* **2002**, *12*, 1952.
[81] S. Iijima, T. Ichihashi, *Nature* **1993**, *363*, 603.
[82] S. Iijima, *Nature* **1991**, *354*, 56.
[83] B. M. Kim, A. M. S. Fuhrer, *J. Phys.: Condens. Matter* **2004**, *16*, R553.
[84] T. W. Ebbesen, H. J. Lezec, H. Hiura, J. W. Bennett, H. F. Ghaemi, T. Thio, *Nature* **1996**, 382.
[85] M. M. J. Treacy, T. W. Ebbesen, J. M. Gibson, *Nature* **1996**, *381*, 678.
[86] J. P. Salvetat, G. A. D. Briggs, J. M. Bonard, R. R. Bacsa, A. J. Kulik, T. Stockli, L. Forró, *Phys. Rev. Lett.* **1999**, *82*, 944.
[87] K. Balasubramanian, M. Burghard, *Small* **2005**, *1*, 180.
[88] M. Holzinger, O. Vostrowsky, A. Hirsch, F. Hennrich, M. Kappes, R. Weiss, F. Jellen, *Angew. Chem., Int. Ed.* **2001**, *40*, 4002.
[89] K. Fu, W. Huang, Y. Lin, L. A. Riddle, D. L. Carroll, Y. P. Sun, *Nano Lett.* **2001**, *1*, 439.
[90] A. Star, Y. Liu, K. Grant, L. Ridvan, J. F. Stoddart, D. W. Steuerman, M. R. Diehl, A. Boukai, J. R. Heath, *Macromolecules* **2003**, *36*, 553.
[91] C. Ehli, G. M. A. Rahman, N. Jux, D. Balbinot, D. M. Guldi, D. F. Paolucci, M. Marcaccio, D. Paolucci, M. Melle-Franco, F. Zerbetto, S. Campidelli, M. Prato, *J. Am. Chem. Soc.* **2006**, *128*, 11222.
[92] C. C. Yang, Y. C. Lin, P. I. Wang, D. J. Liaw, S. W. Kuo, *Polymer* **2014**, *55*, 2044.
[93] M. G. Mohamed, K. C. Hsu, S. W. Kuo, *Polym. Chem.* **2015**, *6*, 2423.
[94] M. G. Mohamed, C. H. Hsiao, F. Luo, L. Dai, S. W. Kuo, *RSC Adv.* **2015**, *5*, 45201.
[95] C. F. Wang, H. Y. Chen, S. W. Kuo, Y. S. Lai, P. F. Yang, *RSC Adv.* **2013**, *3*, 9764.
[96] C. Zuniga, L. Bounaud, G. Ligadas, J. C. Ronda, M. Galiá, V. Cádiz, P. Dubois, *J. Mater. Chem. A* **2014**, *2*, 6814.
[97] C. Lee, X. D. Wei, J. W. Kysar, J. Han, *Science* **2008**, *321*, 385.
[98] W. Gao, L. B. Alemany, L. J. Li, P. M. Aiayan, *Nat. Chem.* **2009**, *1*, 403.
[99] A. A. Alhwaige, S. M. Alhassan, M. S. Katsiotis, H. Ishida, *RSC Adv.* **2015**, *5*, 92719.
[100] R. S. Kumar, M. Ariraman, M. Alagar, *RSC Adv.* **2015**, *5*, 23787.
[101] Q. Xu, M. Zeng, Z. Feng, D. Yin, Y. Huang, Y. Chen. C. Yan, R. Li, Y. Gu, *RSC Adv.* **2016**, *6*, 31484.

© 2018 WILEY-VCH Verlag GmbH & Co. KGaA, Weinheim